Supporting Information

Probing the interplay between geometric and electronic structure in a two-dimensional K-TCNQ charge transfer network

P. J. Blowey,[a,b] L. A. Rochford,[c] D. A. Duncan,[b] D. A. Warr,[c] T.-L. Lee,[b] D.P. Woodruff,[a] and G. Costantini[c]

a) *Department of Physics, University of Warwick, Coventry, CV4 7AL, UK.*

b) *Diamond Light Source, Harwell Science and Innovation Campus, Didcot, OX11 0QX, UK.*

c) *Department of Chemistry, University of Warwick, Coventry, CV4 7AL, UK.*

[†] *present address: School of Chemistry, University of Birmingham, Birmingham, B15 2TT, UK.*

Bulk K-TCNQ structure

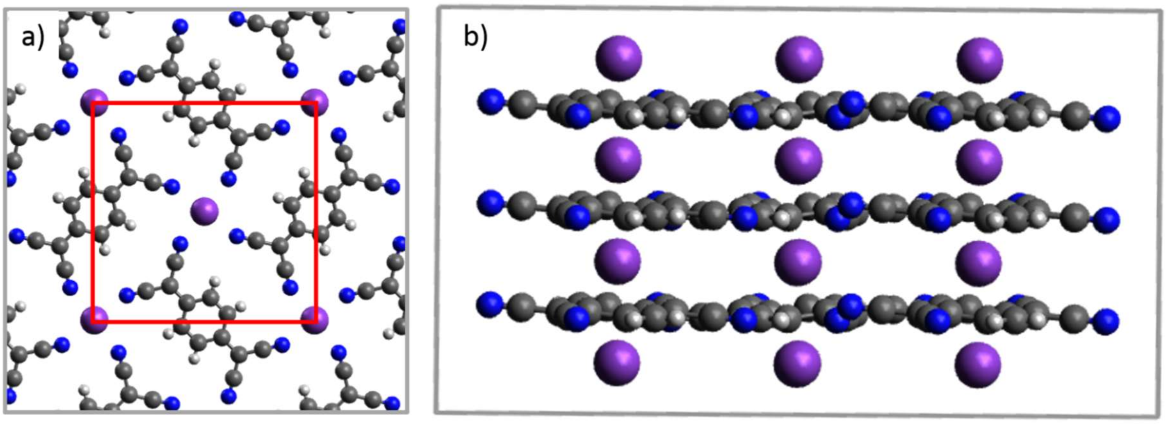

Figure S1 – The 140 °C bulk crystal structure of K-TCNQ[1] showing (a) a top view of the TCNQ layers and (b) a side view displaying the separate layers of TCNQ molecules and K^+ ions.

As described in the main text, bulk crystalline K-TCNQ also contains layers of TCNQ molecules which arrange in a windmill motif about an out-of-plane K^+ ion. Figure S1a shows a visualisation of the 140 °C K-TCNQ bulk crystal structure[1] viewed perpendicular to the (100) plane with a unit mesh analogous to the one for the K-TCNQ surface structure shown as a red square. This 'unit mesh' for the bulk crystal can be described by two vectors of length a = 12.676 Å, b = 12.614 Å with an included angle of 90°. Figure S1b is a side view of the same structure showing the alternating layers of TCNQ molecules and K^+ ions. The layers of K^+ ions are separated from the TCNQ layers by 1.794 Å, with each K^+ ion coordinated by a CN group of 8 different molecules in a cubic arrangement.

Comparison of commensurate and incommensurate LEED patterns

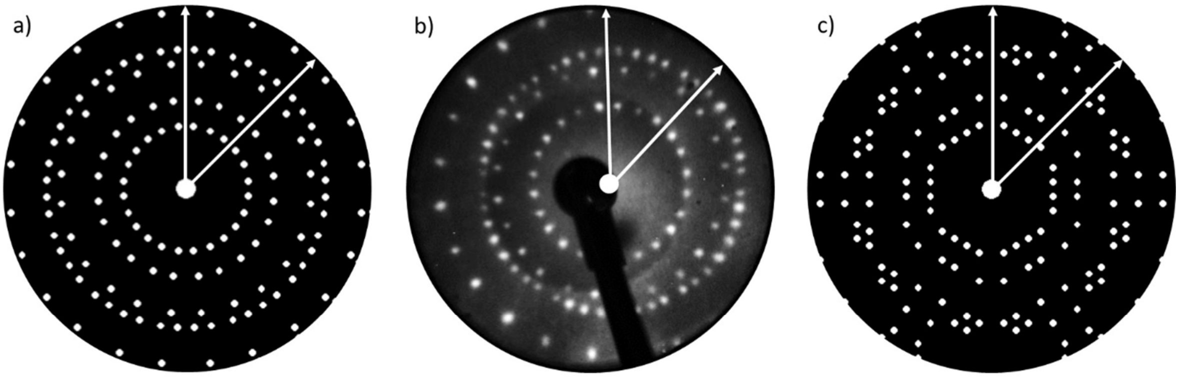

$$\begin{pmatrix} 5.31 & 3.22 \\ -0.65 & 4.28 \end{pmatrix}$$

a = 13.4 Å
b = 13.4 Å
γ = 90 °
Rotated 7° from
substrate unit vectors

a = 13.7 ± 0.4 Å
b = 13.0 ± 0.4 Å
γ = 88 ± 2 °
Rotated 9 ± 2° from
substrate unit vectors

$$\begin{pmatrix} 5.00 & 3.00 \\ -1.00 & 4.00 \end{pmatrix}$$

a = 12.6 Å
b = 13.2 Å
γ = 85.7 °
Rotated 11° from
substrate unit vectors

Figure S2 – (a) Simulated LEED pattern for an incommensurate unit mesh within the error ranges of the STM measured unit mesh. The unit mesh matrix and dimensions are listed below the simulated pattern. (b) The experimental LEED pattern (slightly off normal incidence) for K-TCNQ on Ag(111) at a kinetic energy of 23.5 eV. The STM measured unit mesh dimensions are listed below the pattern. (c) Simulated LEED pattern corresponding to the closest commensurate unit mesh to that measured by STM. The unit mesh matrix and dimensions are listed below the simulated pattern.

Figure S2 compares the LEED pattern observed experimentally for the K-TCNQ networks on Ag(111) alongside two simulated LEED patterns corresponding to an incommensurate and a commensurate unit mesh. The simulated pattern in figure S2a was set to the STM measured unit mesh and was adjusted within the error ranges to give the best agreement to the experimental pattern. The simulated pattern in figure S2c was set to the commensurate structure closest (i.e. the nearest integer values in the matrix representation) to the STM measured unit mesh. This LEED pattern is clearly significantly different from that observed experimentally. In contrast, the pattern simulated using the incommensurate mesh is in excellent agreement with experiment. We therefore conclude that the K-TCNQ network is incommensurate with respect to the underlying Ag(111) substrate.

STM images at varying K exposure

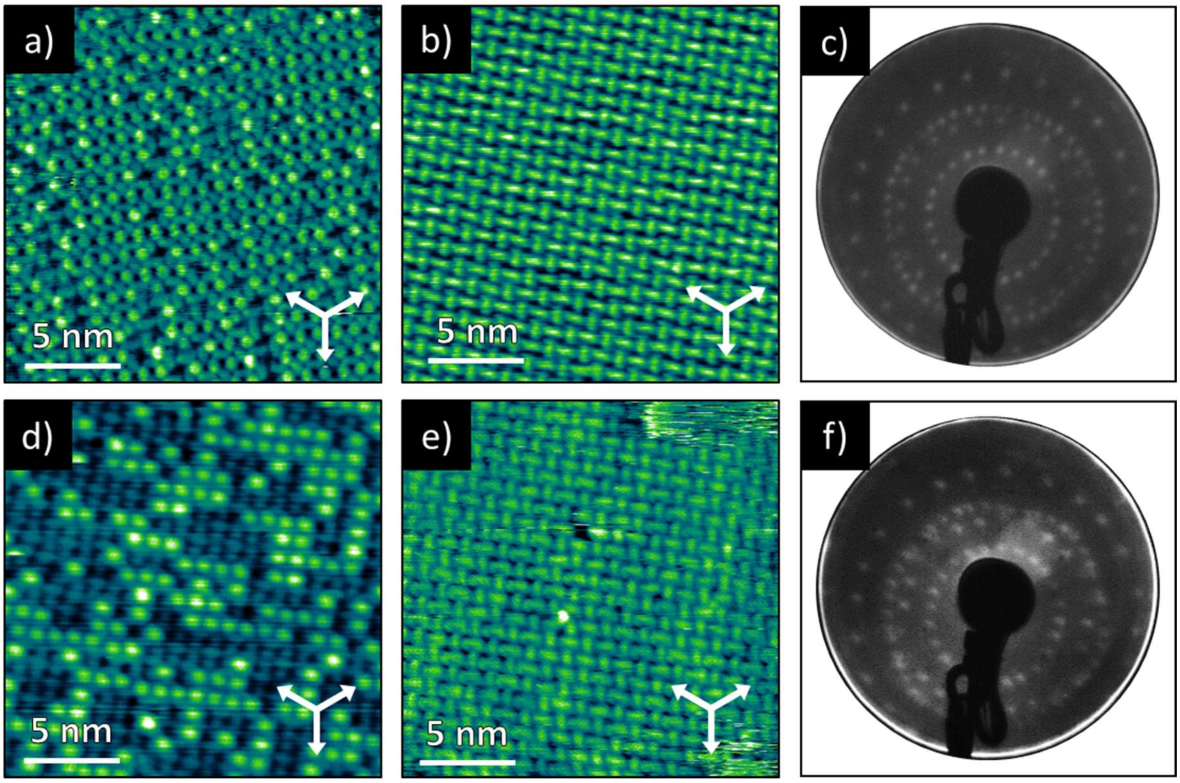

Figure S3 – STM images and LEED patterns obtained for K-TCNQ networks prepared by depositing different amounts of K onto similarly prepared TCNQ/Ag(111) samples. Panels (a-c) correspond to the higher K exposure sample, panels (d-f) to the lower K exposure. The two samples were prepared using K depositions differing by a factor of three. Experimental parameters: (a) and (d) STM images, –1.5 V, 300 pA, (b) STM image, 0.1 V, 175 pA, (c) and (f) LEED patterns at a kinetic energy of 25 eV, (e) STM image, –1.4 V, 60 pA.

Figure S3 shows comparative STM images and LEED patterns from K-TCNQ surface phases formed by depositing two different amounts of K onto similarly prepared TNCQ/Ag(111) samples. Panels (a-c) show experimental data for a sample prepared by depositing K for 6 minutes at a current of 6.3 A and panels (d-f) show data for a 2-minute deposition of K at the same current. For both of these samples, the same periodicity was observed in the STM images and the same LEED pattern was obtained. This indicates that the ordering of the TCNQ was unchanged by the difference in K exposure. STM images taken at a voltage bias of –1.5 V for both samples (figure S3a and S3d) show bright, round protrusions in the STM which we assign to the location of K ions. For the sample subjected to the higher exposure of K, a higher density of these bright features is observed than in the analogous images from the sample exposed to less K. Evidently, lower K exposures lead to the same structural phase but with more vacancies at the K sites. The same ordering is thus observed for a range of different K:TCNQ stoichiometric ratios.

Adjustments to the NIXSW coherent fractions to account for non-linearity in the electron analyser

A problem we have identified in fitting of the C 1s NIXSW absorption profiles in this system, but also seen in other adsorption systems by us and other groups at the I09 beamline of the Diamond Light Source, is exceptionally high values of the coherent fractions, either very close to, or even greater than, unity. A coherent fraction of greater than unity is physically meaningless, and indeed due to thermal vibrations which cause both incoherence in the standing wavefield, but also create a distribution of positions of the adsorbate atoms, coherent fractions at room temperature should not exceed a value of 0.9 on Ag(111) (which has a particularly low Debye temperature). A range of tests to identify the source of this problem have identified the cause as being the non-linear detector response in the VG Scienta EW4000 HAXPES hemispherical electron analyser on the I09 beamline at Diamond Light Source, which impacts on the modulation of the photoemission yield when scanning through the rocking curve. This problem has been previously found to be characteristic of other similar analysers.[2,3] The characteristics of the instrument at I09 are currently being investigated but early tests indicate that the response behaviour is complex, requiring further extremely detailed measurements before a reliable correction methodology can be developed. However, we have conducted a range of tests of highly simplified correction methods that show that the impact of this non-linearity is to significantly increase the apparent coherent fractions but to cause very much smaller changes to the coherent position that appear to fall within usual precision estimates of the measurements.

Based on this evaluation we have applied a 10% reduction to all the coherent fraction values obtained from fitting the NIXSW profiles measured in this investigation; these reduced values are the ones reported in the manuscript. The coherent positions have not been changed. This 10% reduction brings the highest reported coherent fractions values down to 0.90, the highest physically reasonable value. In recognition of this somewhat arbitrary procedure we have increased the reported uncertainty estimates of the coherent fractions to include the original (high) measured values. These larger uncertainty estimates also cover somewhat lower coherent fractions that would be obtained by an even larger adjustment to the measured values. The unadjusted NIXSW fitting parameters are shown in table S1.

	K-TCNQ		TCNQ only[4]		K only	
	f	P	*f*	P	*f*	P
K	0.79(5)	0.51(1)	-	-	0.82(4)	0.19(1)
CH	1.00(2)	0.21(1)	0.95(4)	0.21(1)	-	-
CC	1.00(2)	0.19(1)	0.99(2)	0.18(1)	-	-
CN	0.91(2)	0.18(1)	0.89(3)	0.17(1)	-	-
N	0.41(1)	0.18(2)	0.39(6)	0.17(1)	-	-

Table S1 – NIXSW fitting parameters (coherent fraction f and fractional coherent position P) for the K-TCNQ phase, TCNQ on Ag(111)[4], and K on Ag(111). The quoted values are averaged from a minimum of three separate measurements, with the variations across the measurements quoted as the uncertainty.

Relative K to TCNQ coverage using the K 2p and C 1s SXPS signals

The relative coverages of TCNQ and K were determined by comparing the photoemission intensities of the C 1s and K 2p core levels and accounting for the differences in photoemission cross-sections.

The cross-sections were corrected for the angular distribution of photoemission by using:

$$\sigma_{corrected} = \sigma_i(1 + \beta P_2(\cos\theta)),$$

where σ_i is the photoemission cross-section, β is the dipole asymmetry parameter, $P_2(\cos\theta)$ is the second order Legendre polynomial and θ is the angle between the photon polarisation vector and the photoelectron emission direction which, for the experimental geometry used here, was 0°. Expanding $P_2(\cos\theta)$ and substituting 1 for cos(0) the equation then gives:

$$\sigma_{corrected} = \sigma_i(1 + \beta).$$

In order to normalise, the integrated photoemission peak intensities are then divided by the respective corrected cross sections. To account for each TCNQ molecule containing 12 C atoms, the C 1s intensity was also divided by 12.

$I_{normalised} = \frac{I}{\sigma_{corrected} \times n}$,where $I_{normalised}$ is the peak intensity normalised for cross-section, asymmetry and number of atoms per molecule, I is the integrated photoemission peak intensity and n is the number of atoms of a given element per molecule (where applicable).

The values described above have been tabulated below for the K 2p and the C 1s core levels. These values correspond to a photon energy of 435 eV. Cross-sections and dipole parameters were obtained from atomic and nuclear data tables.[5,6]

	K 2p	C 1s
I	39.7	189.6
σ_i / Mbarn	1.51	0.380
β	1.34	2.00
$\sigma_{corrected}$ / Mbarn	3.53	1.14
n (atoms per molecule)	N/A	12
$I_{normalised}$	11.2	13.9
Ratio	0.81	1.00

The data suggests that there are 0.81 K atoms per TCNQ molecule on the surface.

References

1. M. Konno, T. Ishii and Y. Saito, *Acta Crystallogr. Sect. B: Struct. Sci.*, 1977, **33**, 763-770.
2. N. Mannella, S. Marchesini, A. W. Kay, A. Nambu, T. Gresch, S. H. Yang, B. S. Mun, J. M. Bussat, A. Rosenhahn and C. S. Fadley, *J. Electron. Spectrosc. Relat. Phenom.*, 2004, **141**, 45-59.
3. T. J. Reber, N. C. Plumb, J. A. Waugh and D. S. Dessau, *Rev. Sci. Instrum.*, 2014, **85**, 043907.
4. P. J. Blowey, S. Velari, L. A. Rochford, D. A. Duncan, D. A. Warr, T.-L. Lee, A. De Vita, G. Costantini and D. P. Woodruff, to be published.
5. J.-J. Yeh, *Atomic calculation of photoionization cross-sections and asymmetry parameters*, Gordon & Breach Science Publishers, 1993.
6. J. J. Yeh and I. Lindau, *At. Data Nucl. Data Tables*, 1985, **32**, 1-155.